Modes of collisional orogenic growth: forward, backward and thermally induced

Nuno Rodrigues[1,2], Nicolas Riel [3], Filipe Rosas[1,2], Jaime Almeida[4,5], Afonso Gomes[1,2], João Duarte[1,2]

(1) - Departamento de Geologia, Faculdade de Ciências, Universidade de Lisboa, Portugal
(2) - Instituto Dom Luiz (IDL), Faculdade de Ciências, Universidade de Lisboa, Portugal
(3) - Institute for Geosciences, Johannes Gutenberg-Universität Mainz, Mainz, Germany
(4) - Instituto Dom Luiz (IDL), Universidade da Beira Interior, Portugal
(5) - SEGAL, Departamento de Informática da Universidade da Beira Interior, Portugal

This presentation participates in OSPP

Outstanding Student & PhD candidate Presentation contest

Introduction

This work aims at understanding **orogenic dynamics** and how they can be developed by different processes.

Orogenic plateau formation requires some form of overriding continent deformation or delamination processes. The transition from wedges (narrow and triangular in shape) to plateaus (wide and pancake shaped) have been attributed, among others, to channel flow (Bird, 1991), injection of colliding continent lower crust onto the upper continent (England & Mckenzie, 1982; Zhao & Morgan, 1987), or to lithospheric delamination processes (as compiled by Göğüş & Ueda (2018), and references therein). Despite this, the dynamic factors that govern orogenic growth and the promotion of orogenic wedges and orogenic plateaus are still poorly understood.

Thus, in a **buoyancy-driven** framework of continued continental subduction, we explore how **crustal rheology** controls the development of different **types of orogenic growth**. Without the need of external forces driving the collisional system, we identify three types of orogenic growth (**forward**, **backward** and **thermally induced**) which are highly dependent on crustal rheology.

Model Setup

Using **LaMEM** (Kaus et al., 2016) coupled with **MAGEMin** (Riel et al., 2022) 2D buoyancy driven numerical models of continental collision were developed.

Domain was set to 6000 x 700 km (discretized by 2048 x 256 nodes grid);

The **rheological structure of the continental crust** was modified from strong to very weak (see Fig.1). The effect of water in the **density** of the lower crust was also tested (0 wt%, 1.5wt%, 3wt%, 5 wt% and 10 wt%).

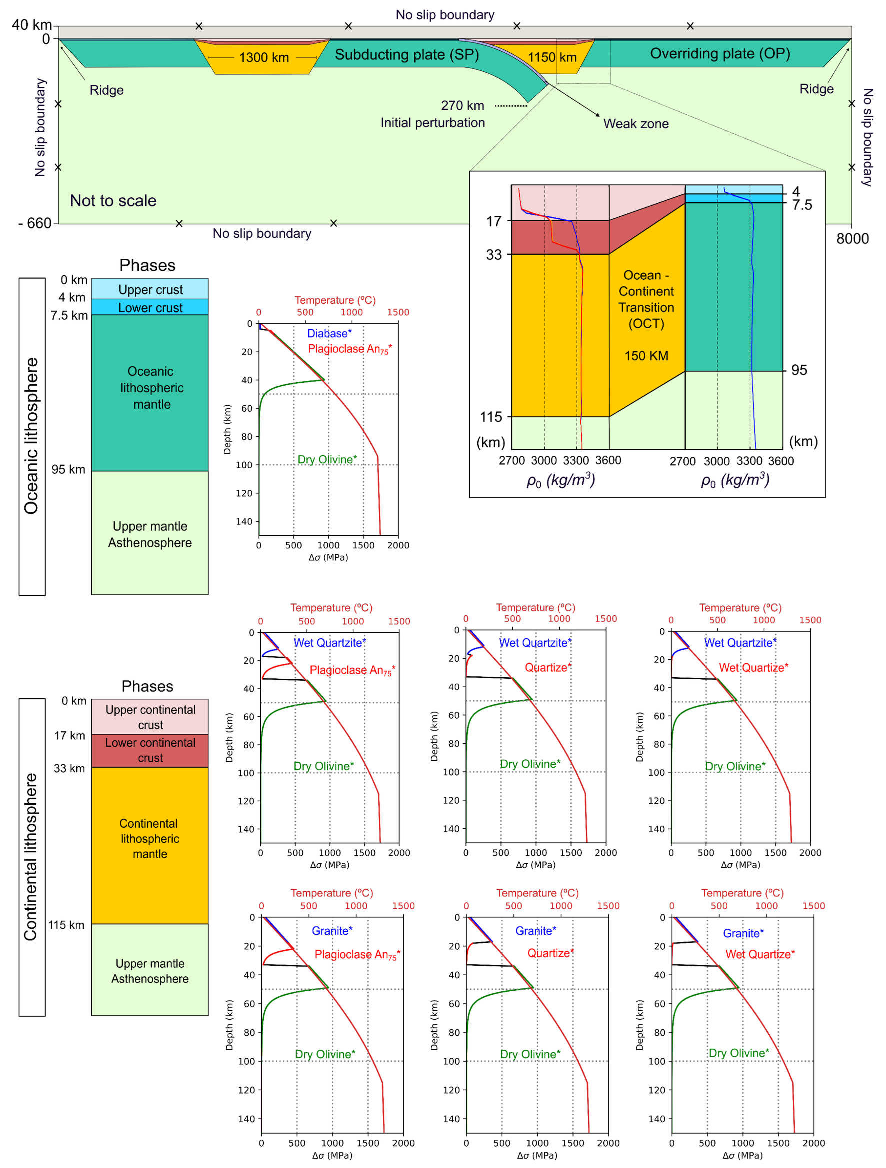

Fig.1 – Model setup for the initial state: schematic representation of the model dimensions and geometric configuration, boundary conditions and overall rheological structure with yield strength envelopes (YSE) for each experiment. Yield strength envelopes were calculated for a background strain rate of 10−15 and based on the type of tensor correction necessary, following Gerya (2019).

Table 1 – Experiments table depicting all explored variables and main findings.

Experiment	Lower Crust	Upper Crust	Water content (Lower crust)	Comments
1	**Weak**: Quartzite (Disl)[1]	**Very weak**: Wet Quartzite (Disl)[1]	0 wt%	Forward orogenic growth; Development of a large-scale lower crustal detachment connecting both continents
2	**Weak**: Quartzite (Disl)[1]	**Very weak**: Wet Quartzite (Disl)[1]	1.5 wt%	
3	**Weak**: Quartzite (Disl)[1]	**Very weak**: Wet Quartzite (Disl)[1]	3 wt%	
4	**Weak**: Quartzite (Disl)[1]	**Very weak**: Wet Quartzite (Disl)[1]	5 wt%	
5	**Weak**: Quartzite (Disl)[1]	**Very weak**: Wet Quartzite (Disl)[1]	10 wt%	
6	**Weak**: Quartzite (Disl)[1]	**Strong**: Granite (Disl)[2]	0 wt%	
7	**Weak**: Quartzite (Disl)[1]	**Strong**: Granite (Disl)[2]	1.5 wt%	
8	**Weak**: Quartzite (Disl)[1]	**Strong**: Granite (Disl)[2]	3 wt%	
9	**Weak**: Quartzite (Disl)[1]	**Strong**: Granite (Disl)[2]	5 wt%	
10	**Weak**: Quartzite (Disl)[1]	**Strong**: Granite (Disl)[2]	10 wt%	
11	**Very weak**: Wet Quartzite (Disl)[1]	**Very weak**: Wet Quartzite (Disl)[1]	0 wt%	
12	**Very weak**: Wet Quartzite (Disl)[1]	**Very weak**: Wet Quartzite (Disl)[1]	1.5 wt%	
13	**Very weak**: Wet Quartzite (Disl)[1]	**Very weak**: Wet Quartzite (Disl)[1]	3 wt%	
14	**Very weak**: Wet Quartzite (Disl)[1]	**Very weak**: Wet Quartzite (Disl)[1]	5 wt%	
15	**Very weak**: Wet Quartzite (Disl)[1]	**Very weak**: Wet Quartzite (Disl)[1]	10 wt%	
16	**Very weak**: Wet Quartzite (Disl)[1]	**Strong**: Granite (Disl)[2]	0 wt%	
17	**Very weak**: Wet Quartzite (Disl)[1]	**Strong**: Granite (Disl)[2]	1.5 wt%	
18	**Very weak**: Wet Quartzite (Disl)[1]	**Strong**: Granite (Disl)[2]	3 wt%	
19	**Very weak**: Wet Quartzite (Disl)[1]	**Strong**: Granite (Disl)[2]	5 wt%	
20	**Very weak**: Wet Quartzite (Disl)[1]	**Strong**: Granite (Disl)[2]	10 wt%	
21	**Strong**: Plagioclase An_{75} (Disl)[1]	**Very weak**: Wet Quartzite (Disl)[1]	0 wt%	Backward orogenic growth; No large-scale lower crustal detachment is formed
22	**Strong**: Plagioclase An_{75} (Disl)[1]	**Very weak**: Wet Quartzite (Disl)[1]	1.5 wt%	
23	**Strong**: Plagioclase An_{75} (Disl)[1]	**Very weak**: Wet Quartzite (Disl)[1]	3 wt%	
24	**Strong**: Plagioclase An_{75} (Disl)[1]	**Very weak**: Wet Quartzite (Disl)[1]	5 wt%	
25	**Strong**: Plagioclase An_{75} (Disl)[1]	**Very weak**: Wet Quartzite (Disl)[1]	10 wt%	
26	**Strong**: Plagioclase An_{75} (Disl)[1]	**Strong**: Granite (Disl)[2]	0 wt%	Thermally induced orogenic growth; Peel back delamination after slab break-off
27	**Strong**: Plagioclase An_{75} (Disl)[1]	**Strong**: Granite (Disl)[2]	1.5 wt%	
28	**Strong**: Plagioclase An_{75} (Disl)[1]	**Strong**: Granite (Disl)[2]	3 wt%	
29	**Strong**: Plagioclase An_{75} (Disl)[1]	**Strong**: Granite (Disl)[2]	5 wt%	
30	**Strong**: Plagioclase An_{75} (Disl)[1]	**Strong**: Granite (Disl)[2]	10 wt%	
Sensibilty test #1	SP - **Very weak**: Wet Quartzite (Disl)[1]; OP - **Strong**: Plagioclase An_{75}(Disl)[1]	**Very weak**: Wet Quartzite (Disl)[1]	3 wt%	Backward orogenic growth; No large-scale lower crustal detachment is formed
Sensibilty test #2	SP - **Strong**: Plagioclase An_{75}(Disl)[1]; OP - **Very weak**: Wet Quartzite (Disl)[1]	**Very weak**: Wet Quartzite (Disl)[1]	3 wt%	Forward orogenic growth; Development of a large-scale lower crustal detachment connecting both continents

Modes of Orogenic Growth and Topographic response

***Weak** lower crust* ---- *Detachment develops* ---- *Overriding continent deformation*

→ ***Strong** upper crust* ---- *High resistance* ---- **Forward growth**
→ ***Weak** upper crust* ---- Low resistance ---- **Forward growth**

vs.

***Strong** lower crust* ---- *No detachment* ---- *No overriding continent deformation*

→ ***Strong** upper crust* ---- High resistance ---- **Thermally induced growth**
→ ***Weak** upper crust* ---- Low resistance ---- **Backward growth**

Forward orogenic growth

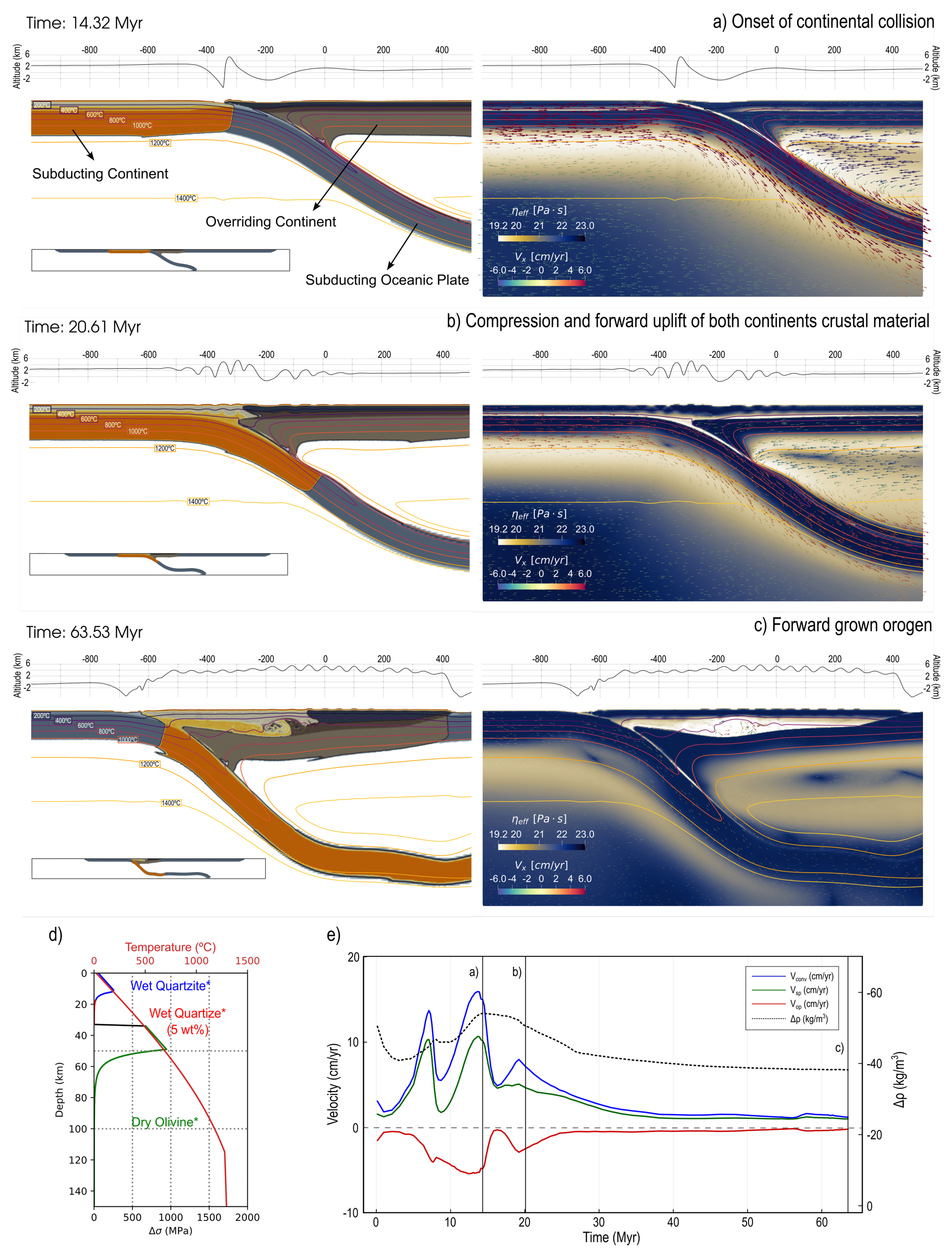

Fig.2. Reference model evolution (experiment #14) of the forward orogenic growth mode, depicting altitudes, phases (left), isotherms, viscosity (right) and velocities (right).

Backward orogenic growth

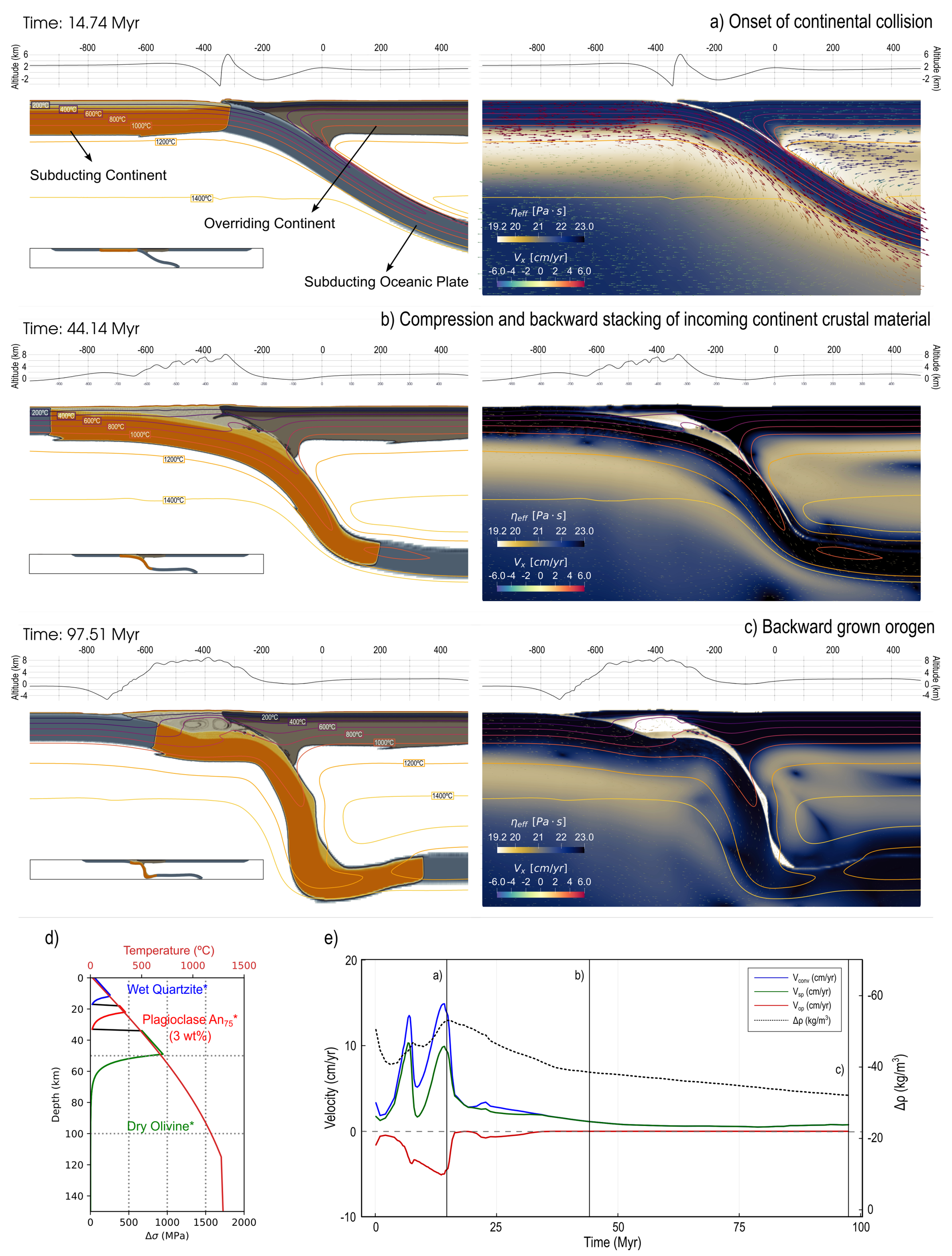

Fig.3. Reference model evolution (experiment #23) of the backward orogenic growth mode, depicting altitudes, phases (left), isotherms, viscosity (right) and velocities (right).

Thermally induced orogenic growth

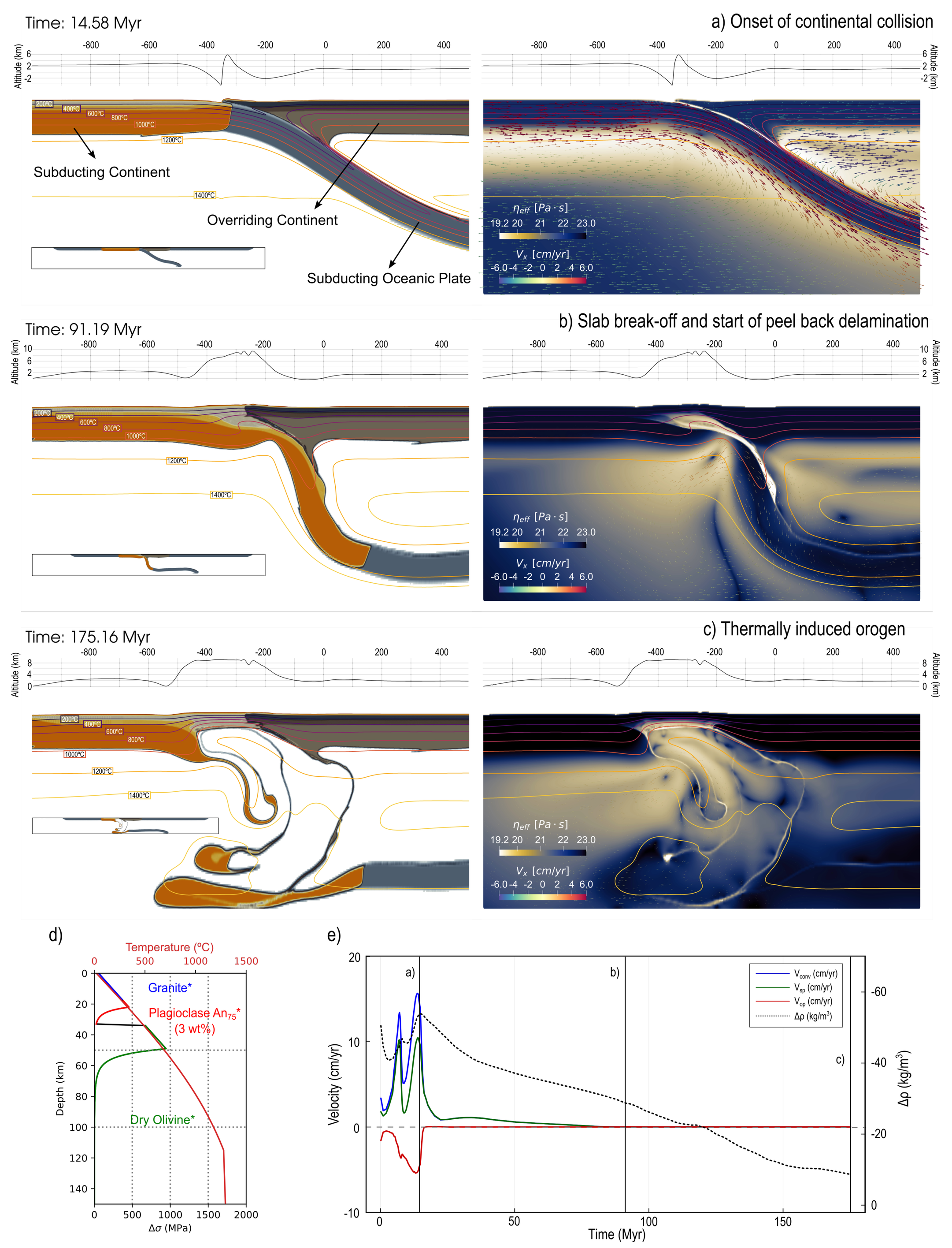

Fig.4. Reference model evolution (experiment #28) of the thermally induced orogenic growth mode, depicting altitudes, phases (left), isotherms, viscosity (right) and velocities (right).

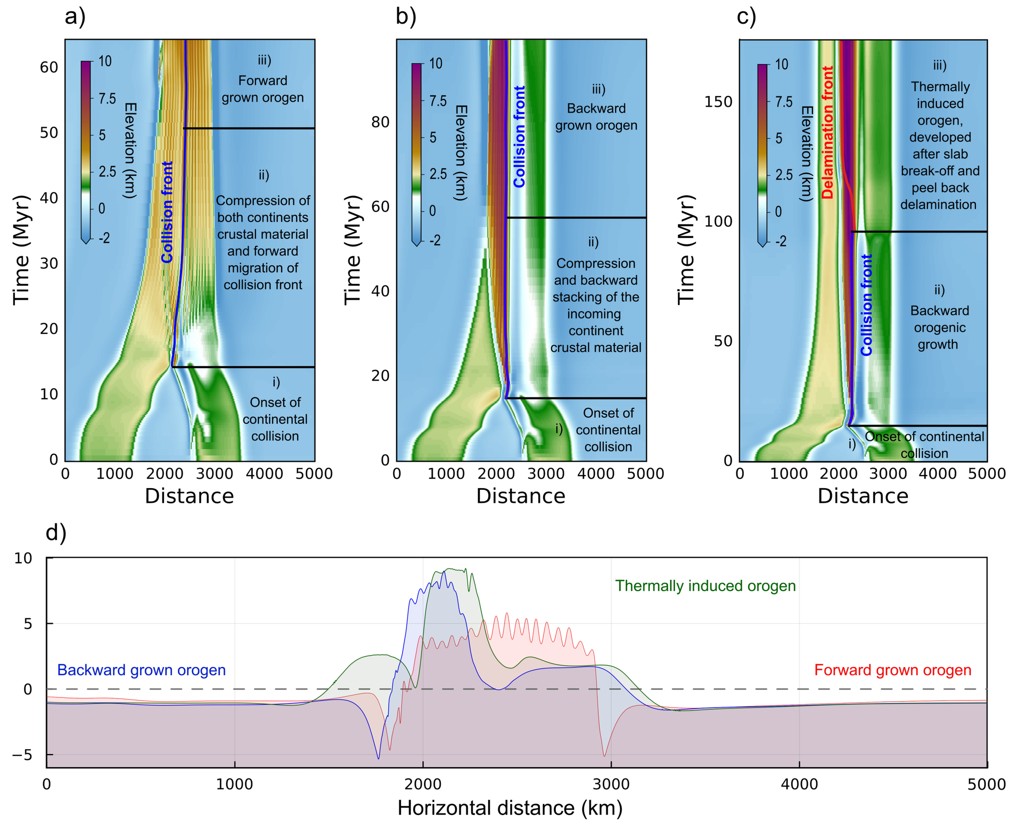

Fig.5. Topographic evolution of reference models presented in Fig.2, 3 and 4 (experiments #14, #23 and #28), and their respective topographic profiles at final stages. a) forward orogenic growth mode reference model; b) backward orogenic growth mode reference model; c) thermally induced orogenic growth mode reference model; d) topographic profiles for reference models in their last stage of evolution (63.53 Myr, 97.51 Myr and 175.16 Myr, respectively)

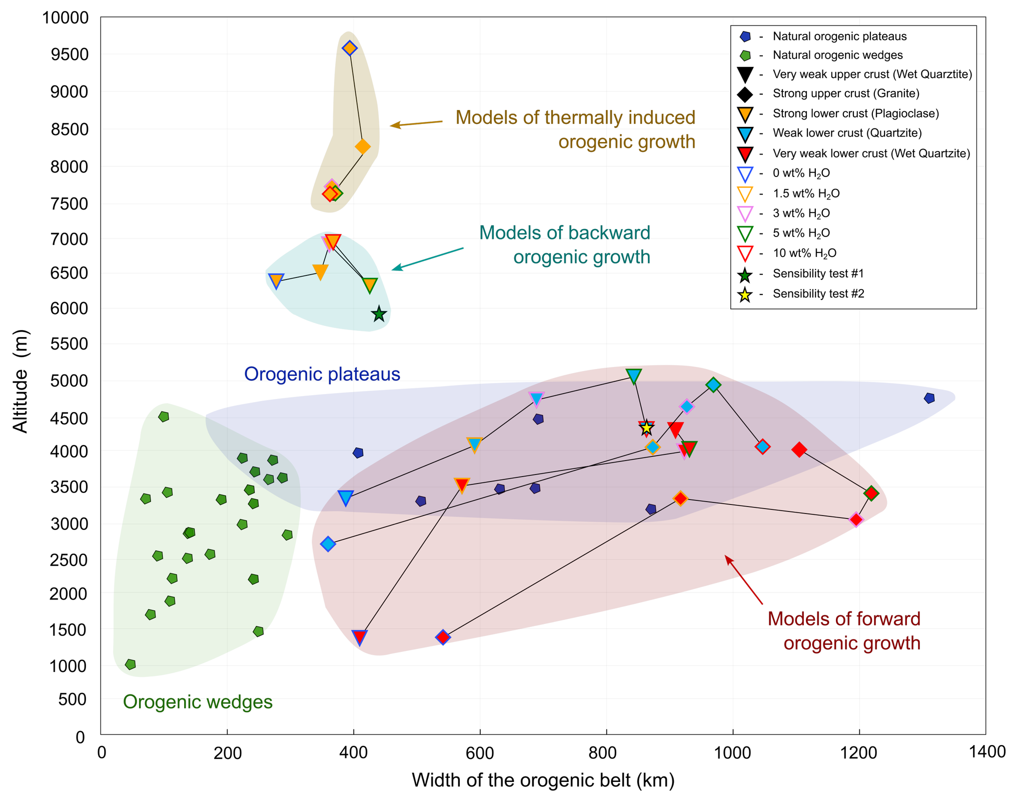

Fig.6. Topography of natural orogens and experimental results. Model mean altitudes are calculated between the most distant points above 2500 meters. Black lines are shown for visual clarity, representing the evolution of width and altitude between models with different water content in the dioritic lower crust. Modified after Vanderhaeghe (2012).

Limitations and further investigation

Limitations:

1st - Lack of toroidal flow (2D modelling framework);

2nd - Lack of surface processes;

3rd - Instantaneous phase changes.

Current research directions (3D modelling):

- Role of toroidal mantle flow in the dynamics of collisional systems;

- Influence of lateral (across width) rheological contrasts in orogenic architecture.

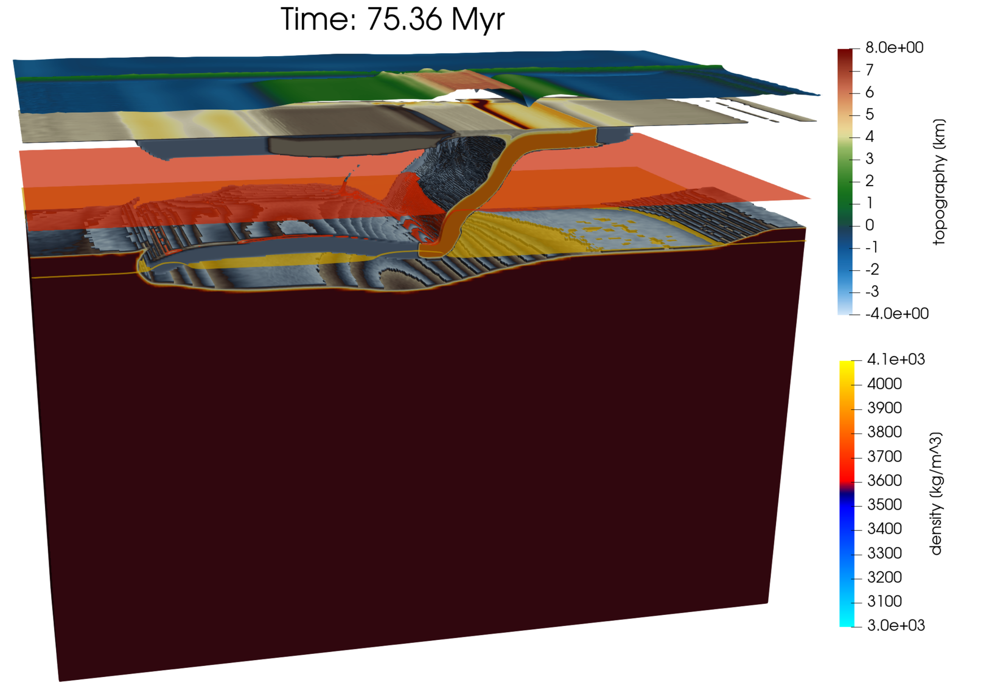

Main takeways

Continued continental subduction and **collision** were achieved in a **buoyancy-driven framework**;

Crustal rheology controls orogenic architecture;

Three modes of orogenic growth were identified: **forward, backward and thermally induced.**

Acknowledgments and references

This work was funded by the Portuguese Fundação para a Ciência e a Tecnologia (FCT) I.P./MCTES through national funds (PIDDAC) – UIDB/50019/2020 (https://doi.org/10.54499/UIDB/50019/2020), UIDP/50019/2020 (https://doi.org/10.54499/UIDP/50019/2020) and LA/P/0068/2020 (https://doi.org/10.54499/LA/P/0068/2020).

References:

Bird, P. (1991). Lateral extrusion of lower crust from under high topography, in the isostatic limit. Journal of Geophysical Research, 96(B6). https://doi.org/10.1029/91jb00370

England, P., & Mckenzie, D. (1982). A thin viscous sheet model for continental deformation. In Geophys J. R. astr. Soc (Vol. 70). https://academic.oup.com/gji/article/70/2/295/557795

Gerya, T. (2019). Introduction to Numerical Geodynamic Modelling (2nd ed.). Cambridge University Press. https://doi.org/DOI: 10.1017/9781316534243

Göğüş, O. H., & Ueda, K. (2018). Peeling back the lithosphere: Controlling parameters, surface expressions and the future directions in delamination modeling. In Journal of Geodynamics (Vol. 117, pp. 21–40). Elsevier Ltd. https://doi.org/10.1016/j.jog.2018.03.003

Kaus, B. J. P., Popov, A. A., Baumann, T. S., Püsök, A. E., Bauville, A., Fernandez, N., & Collignon, M. (2016). Forward and inverse modelling of lithospheric deformation on geological timescales. NIC Symposium 2016 - Proceedings. NIC Series., 48, 299–307. hdl.handle.net/2128/9842

Riel, N., Kaus, B. J. P., Green, E. C. R., & Berlie, N. (2022). MAGEMin, an Efficient Gibbs Energy Minimizer: Application to Igneous Systems. Geochemistry, Geophysics, Geosystems, 23(7). https://doi.org/10.1029/2022GC010427

Vanderhaeghe, O., Medvedev, S., Fullsack, P., Beaumont, C., & Jamieson, R. A. (2003). Evolution of orogenic wedges and continental plateaux: insights from crustal thermal–mechanical models overlying subducting mantle lithosphere. Geophysical Journal International, 153(1), 27–51. https://doi.org/10.1046/j.1365-246X.2003.01861.x

Zhao, W.-L., & Morgan, W. J. (1987). Injection of Indian crust into Tibetan lower crust: A two-dimensional finite element model study. Tectonics, 6(4), 489–504. https://doi.org/https://doi.org/10.1029/TC006i004p00489